PHILOSOPHICAL TRANSACTIONS A

rsta.royalsocietypublishing.org

Research

Cite this article: Arbol PMR, Garcia PG, Gonzalez CD, OrioAlonso A. 2019 Non-destructive testing of industrial equipment using muon radiography. *Phil. Trans. R. Soc. A* **377**: 20180054.
http://dx.doi.org/10.1098/rsta.2018.0054

Accepted: 23 October 2018

One contribution of 21 to a Theo Murphy meeting issue 'Cosmic-ray muography'.

Subject Areas:
high energy physics

Keywords:
muon tomography, muography, muon radiography, industrial inspection, NDT

Author for correspondence:
Carlos Diez Gonzalez
e-mail: carlos@muon.systems

Non-destructive testing of industrial equipment using muon radiography

Pablo Martinez Ruiz-del Arbol[1], Pablo Gomez Garcia[2], Carlos Diez Gonzalez[2] and Aitor OrioAlonso[2]

[1]Physics Institute of Cantabria (IFCA), University of Cantabria, Santander, Spain
[2]Muon Tomography Systems S. L. Vasque country, Spain

PMRA, 0000-0002-7737-5121

A new application of muon radiography (MR) is presented in the context of non-destructive testing of industrial equipment. The long-term operation of industrial facilities frequently involves the deterioration of critical components such as pipes and cauldrons due to corrosion and other processes. The precise determination of the inner state of this equipment is needed to ensure the integrity of the facility. MR can be used to infer the thickness of these components through the comparison and further classification of muon observables with respect to well-known templates. A simulation example is presented where the thickness of a pipe made of steel is studied using the Point of Closest Approach method and simple Kolmogorov–Smirnov statistical tests. A precision of about 2–4 mm is obtained using a simple detector with a spatial resolution of 4 mm and exposure times of about 2 h.

This article is part of the Theo Murphy meeting issue 'Cosmic-ray muography'.

1. Introduction

In 1912, Victor Hess initiated a series of balloon-flights over the roofs of Vienna to measure the intensity of the radiation in the atmosphere at different heights. He found that radiation was more intense at greater altitudes and concluded that the Earth was being bombarded by a flux of particles. These particles are nowadays known as cosmic rays and they are known to be composed mainly of protons which often interact with the atoms of the atmosphere producing large cascades

THE ROYAL SOCIETY PUBLISHING

of particles. Most of these products are quickly absorbed by the atmosphere, although some others, such as the muons, are able to propagate to the surface of the Earth before decaying or being absorbed. Precise measurements of the flux of cosmic muons at different altitudes including the Earth's surface can be found in [1].

Muons are subatomic particles sharing the properties of the electrons and about 200 times heavier than them. Since they are charged particles, they undergo electromagnetic interactions with the atoms of the material they cross in two interesting ways: losing energy through ionization of the material, or being deflected as a result of the multiple scattering with the material nuclei. Both processes have a strong dependency on the properties of the crossed medium such as the density, the atomic number or the number of radiation lengths, providing a powerful handle to identify its size, shape and composition. This fact enabled the possibility of measuring the attenuation or the bending of the muons when crossing an object to infer details about its geometry. This technique is nowadays known as muon radiography (MR). The first effort in developing this technology was made in the context of underground applications using attenuation [2]. Other applications have been published using also the muon deviation pattern [3].

MR applications involve two different developments: the manufacturing of muon detectors and the algorithmic reconstruction of the target geometry. Muon detectors frequently use the ionization of the muons when crossing their active material to determine its position. Different materials are used for this purpose being the most common gas, scintillators and silicon cells. All of them require a readout electronic system that is able to extract and digitize the signal. Reconstruction algorithms strongly depend on the application and physical principle considered. For those applications using the muon deflection several algorithms are available on the market. One of the most popular, because of its simplicity and efficiency, is the Point of Closest Approach (POCA) [4]. This algorithm assumes that the interaction of the muon with the object takes place in a single spatial point, determined as the point of closest approach between the incoming and outgoing trajectories. There are other algorithms with a higher sophistication such as the maximum-likelihood method [5], or others using autocorrelation methods [6].

This paper presents a new MR application focused on the preventive maintenance of industrial facilities. Important sectors of the economy such as the steel or the petroleum industries are affected by the corrosion of insulated equipment [7–10] like pipes, cauldrons or blast furnaces. The maintenance of this equipment has a high cost in terms of energy and money, especially when the production of the factory has to be partially or totally stopped. Nowadays different technologies are used to address this problem, however all of them imply the removal of the insulation layer or the use of ionizing radiation, resulting in a large economic impact. This work proposes MR as a method to assess information about the integrity of insulated equipment without stopping the production process. The novelty of this study relies on the application of MR as a problem of classification in which muon observables are compared using well-known templates to find the best match. This procedure seems suitable for systems where the nominal geometry is known with high precision and only small variations with respect to this geometry are being targeted.

2. Geometry description and detector layout

This study applies MR to a cylindrical, steel-made pipe with an outer radius of 20 cm and an inner radius varying from 5 to 19 cm in steps of 2 cm, and from 17.4 to 18.8 cm in steps of 0.2 cm. The length of the pipe is 80 cm. The origin of coordinates is located at the geometrical centre of the cylinder. The x-axis is defined as parallel to the ground and coincident with the cylinder axis, while the z-axis is defined as parallel to the normal.

The muon detector layout contains four hybrid multiwire–multistrip chambers composed by two active planes separated by a distance of 5 mm. One plane is formed by 50 µm-width, gold-tungsten wires every 4 mm, while the second is made of 4 mm copper strips oriented orthogonally to the wires. The combination of the two planes provides a simultaneous measurement of the x- and y-coordinates. The size of the active detection area is $96 \times 96\,\mathrm{cm}^2$ for each plane. Two chambers are located above the pipe at positions $z = 45$ cm and $z = 28$ cm and two chambers are

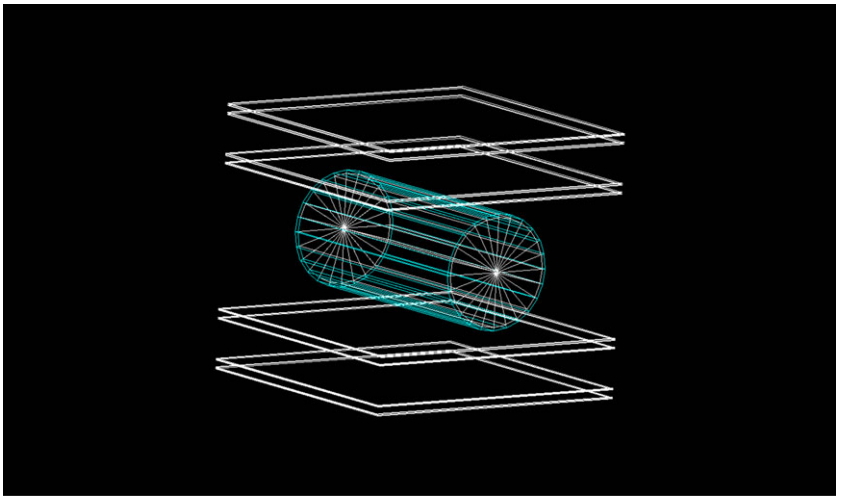

Figure 1. Geometry set-up including the pipe and the detector layout. Only the detection planes are shown in this figure. (Online version in colour.)

located below the pipe at positions $z = -45$ cm and $z = -28$ cm. All the chambers are oriented orthogonal to the z-axis. A sketch of the global set-up can be seen in figure 1. It is worth mentioning that this set-up simulates the chambers being constructed at the facilities of muon systems [11]. The study presented in this report is based exclusively on simulation.

3. Simulation and data samples

Simulated samples are produced using the Cosmic Ray Shower Library (CRY) [12], which generates correlated cosmic-ray particle shower distributions at the sea level. The radiation volume for this simulation has been fixed to $1 \times 1 \times 1\,\mathrm{m}^3$ cube in which the geometry set-up is fully embedded. Generated muons are interfaced to GEANT4 [13] to simulate the interaction of the muons with the detector and the geometry. The detector has been simulated assuming a perfect efficiency of 100% and a resolution of 4 mm to account for the granularity of the active elements (wires and strips). The hits in the individual upper and lower chambers are combined using a linear fit, providing a set of four coordinates each: the x- and y-positions and the two corresponding angular projections.

The generated samples are produced with an exposure time of 6900 s. A total of 16 categories of samples have been generated according to the pipe inner radius. Two equivalent samples have been produced for each category: one is used to produce the template sample, while the other is used as a test sample. The first eight categories consider a thickness in the range 5–15 cm where the amount of material is large and the technique is expected to work well. The other eight categories focus on a thickness range of 1.2–2.6 cm where the discrimination power should be reduced.

4. Results and discussion

The starting point of this procedure uses the three-dimensional distribution of scattering centres provided by the POCA algorithm. The wear of the pipe wall is assumed to be uniform in the longitudinal coordinate in such a way that the x-coordinate of the scattering centres is collapsed in a single plane. In order to remove contamination from random scattering centres in the air, only events with an angular deviation greater than 0.05 rad are selected. The resulting two-dimensional distributions can be seen in figure 2 for a few different-thickness pipes.

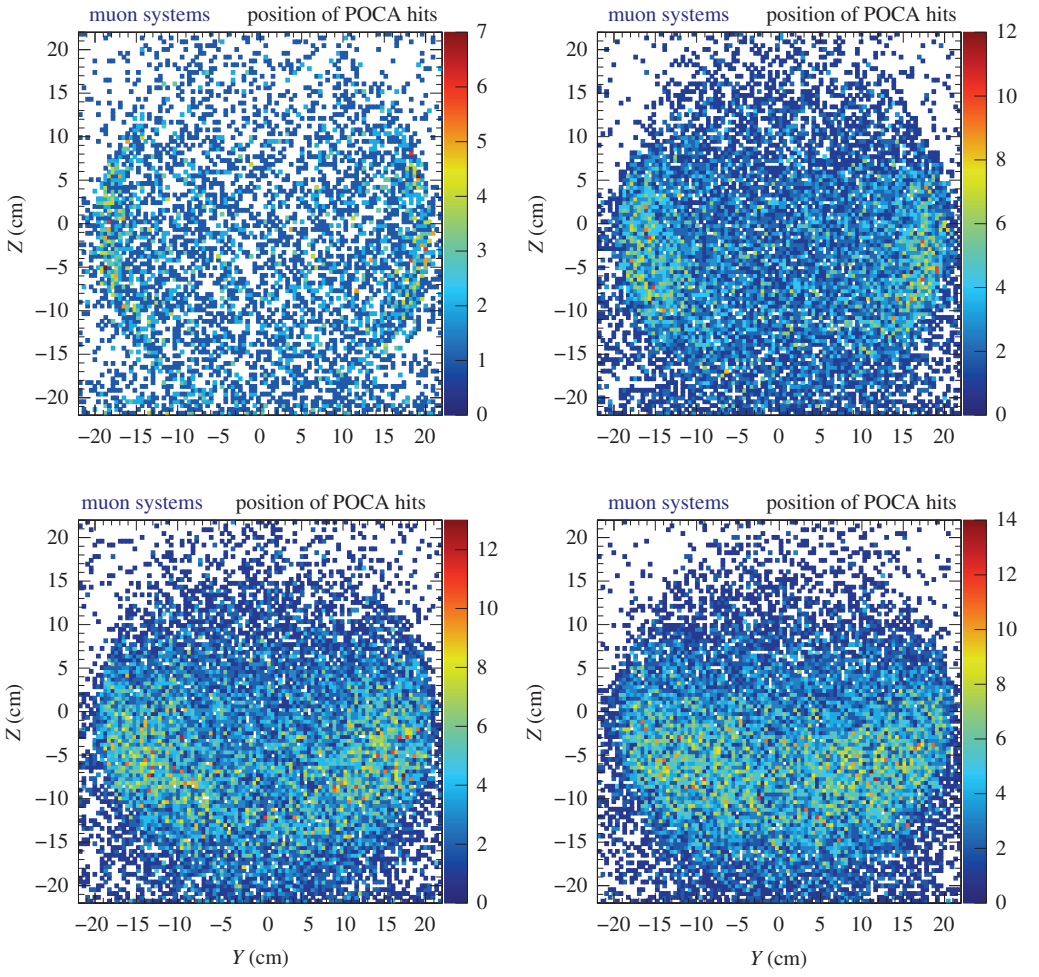

Figure 2. POCA scattering centres projected on the *y*–*z*-plane for different-thickness pipes. From left to right and up to down 1 cm, 5 cm, 9 cm and 13 cm.

A first look at the POCA results reveals that the number of events decreases with the thickness of the pipe. This effect is expected since events with a minimum angular deviation are being selected, favouring scenarios with a lower amount of dense material. The total yields can be used as a rough, first indication of a large difference in the material composition of two different samples, but hardly contains any information about the details of the geometry.

The outer shape of the pipe can be clearly recognized although the resolution is better in the region close to $z = 0$ where the acceptance of the detectors is optimal. The inner wall cannot be inferred so easily although a clear trend to accumulate scattering centres in the inner, hollowed part of the pipe is observed for increasing pipe thickness. Most of the scattering centres in this region are produced by muons that cross the pipe two times, invalidating the POCA assumption on the number of interactions, and making the reconstruction of the inner radius a difficult task.

A further assumption on the azimuthal symmetry of the wear suffered by the pipe is considered, allowing the projection of the two-dimensional histograms into one single coordinate: the radius of the POCA scattering centre. The resulting distributions can be seen in figure 3. This projection confirms the fact that the outer pipe face is easy to identify, while the inner face is more difficult, providing a soft gradient towards zero instead of a steep fall at the radial position of the wall.

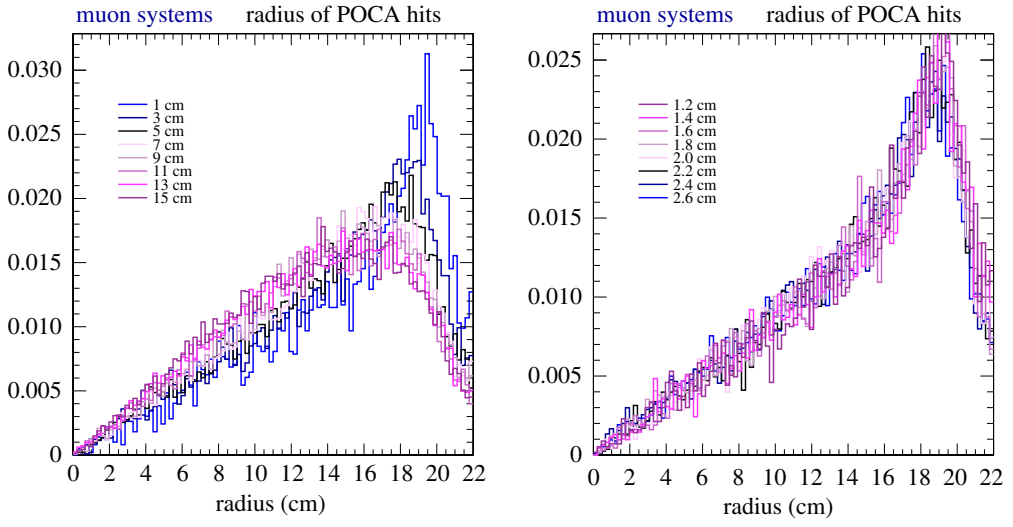

Figure 3. Distributions of the radius of the POCA scattering centres for different pipe thicknesses. The figure on the left contains the distributions for a thickness in the range 5–15 cm, while the figure on the right in the range 1.2–2.6 cm. Distributions are normalized to unit.

Table 1. Scores obtained in the KS test for each test sample and every template. The upper part of the table shows the results for a thickness in the range 5–15 cm, and the lower part the results for a thickness in the range 1.2–2.6 cm.

test/template	1 cm	3 cm	5 cm	7 cm	9 cm	11 cm	13 cm	15 cm
1 cm	0.95	0	0	0	0	0	0	0
3 cm	0	0.80	0	0	0	0	0	0
5 cm	0	0	0.39	0	0	0	0	0
7 cm	0	0	0	0.41	0	0	0	0
9 cm	0	0	0	0	0.29	0	0	0
11 cm	0	0	0	0	0	0.45	0.05	0
13 cm	0	0	0	0	0	0.01	0.86	0.07
15 cm	0	0	0	0	0	0	0	0.48
test/template	1.2 cm	1.4 cm	1.6 cm	1.8 cm	2.0 cm	2.2 cm	2.4 cm	2.6 cm
1.2 cm	0.88	0.73	0.06	0.01	0	0	0	0
1.4 cm	1.00	0.58	0.18	0.01	0	0.01	0	0
1.6 cm	0.04	0.12	0.08	0.81	0.08	0.47	0	0
1.8 cm	0.07	0.14	0.19	0.18	0.35	0.87	0	0
2.0 cm	0.01	0.05	0.67	0.33	0.41	1.00	0.04	0
2.2 cm	0	0	0.01	0.03	0.92	0.14	0.80	0.01
2.4 cm	0	0	0	0.00	0.25	0.01	0.87	0.17
2.6 cm	0	0	0	0.00	0.07	0	0.17	0.57

Even if the reconstruction of the inner wall is not precise, the distributions are different enough to perform statistical tests to check the compatibility between two data samples. It should be noted that obtaining templates for well-known objects is feasible using simulations or by producing dedicated measurements in the laboratory. Once the templates are ready a simple

Kolmogorov–Smirnov test can be performed to classify the target sample. It should be noted that more sophisticated classifiers based on machine learning techniques can be applied directly to the muon observables. This work is currently under investigation.

Table 1 shows the score obtained in the KS test when each of the test samples is compared with every template sample. These numbers show how in most of the cases the best compatibility between a test and a template sample occurs when the thickness of the pipes are coincident. This is strictly true for variations of the order of 2 cm. The cases in which a variation of 0.2 cm was performed are not so clear and some confusion can be observed with the neighbouring templates. A good discrimination at the level of 0.2–0.4 cm can be claimed.

5. Conclusion

This simulation study shows, using a simple mathematical apparatus, how statistical compatibility between muon observables can be used to classify the amount of wear suffered by a steel-made pipe. A simple set-up composed of four hybrid multiwire–multistrip chambers have been considered with a spatial resolution of 4 mm. Pipes with a different thickness have been modelled and MR simulations of 6900 s each have been produced. The distribution of the radius of the POCA scattering centres have been studied and compared to template simulations with different thicknesses. The results show how this procedure is able to discriminate between templates differing by 0.2–0.4 cm. New studies will be carried out to understand what resolution can be obtained with this technique, reducing the symmetry assumptions and using more sophisticated algorithms based on machine learning classifiers.

Authors' contributions. P.M.R.-d.A. conceived the study and performed most of the simulations, figures and mathematical analysis. P.G.G. and P.M.R.-d.A. drafted the manuscript, while C.D.G. and A.O.A. contributed to the preparation and maintenance of the computational infrastructure and have read the analysis and provided useful comments.

Competing interests. The authors declare that they have no competing interests.

Funding. P.M.R.-d.A. is funded by the University of Cantabria through the Ramon y Cajal research program of the Spanish Ministry of Science, Innovation, and Universities. C.D.G., P.G.G. and A.O.A. are funded by Muon Tomography Systems S.L.

Acknowledgements. We would like to thank Fundacion Repsol, Centro para el Desarollo Tecnologico Industrial (CDTI), Spanish Ministry of Science, Innovation, and Universities, and the government of the Vasque Country, for their continuous help and support.

References

1. Patrignani C, Agashe K, Aielli G, Amsler C, Antonelli M, Asner DM, Baer H, Banerjee SW, Barnett RM, Basaglia T (Particle Data Group). 2016 Particle Data Group. *Chin. Phys. C* **40**, 100001. and 2017 update. (doi:10.1088/1674-1137/40/10/100001)
2. George BP. 1955 Cosmic rays measure of overburden of tunnel. *Commonwealth Eng.* **455**, 7.
3. Priedhorsky WC, Borozdin KN, Hogan GE, Morris C, Saunders A, Schultz LJ, Teasdale ME. 2003 Detection of high-Z objects using multiple scattering of cosmic ray muons. *Rev. Sci. Instrum.* **74**, 4294–4297. (doi:10.1063/1.1606536)
4. Riggi S, Antonuccio-Delogu V, Bandieramonte M, Becciani U, Costa A, La Rocca P, Vitello F. 2013 Muon tomography imaging algorithms for nuclear threat detection inside large volume containers with the Muon Portal detector. *Nucl. Instrum. Methods Phys. Res. A, Accel. Spectrom. Detect. Assoc. Equip.* **728**, 59–68. (doi:10.1016/j.nima.2013.06.040)
5. Schultz LJ, Blanpied GS, Borozdin KN, Fraser AM, Hengartner NW, Klimenko AV, Sossong MJ. 2007 Statistical reconstruction for cosmic ray muon tomography. *IEEE Trans. Image Process.* **16**, 1985–1993. doi:10.1109/TIP.2007.901239)
6. Schultz LJ, Borozdin KN, Gomez JJ, Hogan GE, McGill JA, Morris CL, Teasdale ME. 2004 Image reconstruction and material Z discrimination via cosmic ray muon radiography. *Nucl. Instrum. Methods Phys. Res. A, Accel. Spectrom. Detect. Assoc. Equip.* **519**, 687–694. (doi:10.1016/j.nima.2003.11.035)

7. Twomey M. 1997 *Inspection techniques for detecting corrosion under insulation*. United States: N. p., Web.
8. Bray AV, Corley CJ, Fischer RB, Rose JL, Quarry MJ. 1998 Development of guided wave ultrasonic techniques for detection of corrosion under insulation in metal pipe. *Paper presented at Proc. of the 1998 ASME Energy Sources Technology Conf., Houston, TX, USA*. Office of Scientific and Technical Information, US Department of Energy, 31st Dec. 1999.
9. Kwun H, Holt AE. 1995 Feasibility of under-lagging corrosion detection in steel pipe using the magnetostrictive sensor technique. *NDT & E Int.* **28**, 211–214. (doi:10.1016/0963-8695(95)00019-T)
10. Bailey J, Long N, Hunze A. 2017 Eddy current testing with Giant Magnetoresistance (GMR) sensors and a pipe-encircling excitation for evaluation of corrosion under insulation. *Sensors* **17**, 2229. (doi:10.3390/s17102229)
11. Muon Tomography Systems S.L. (n.d.). Retrieved from http://muon.systems/.
12. Chris H, David L, Jerome Verbeke DW. 2012 Cosmic-ray Shower Library (CRY). Retrieved 22 June 2018. See https://nuclear.llnl.gov/simulation/doc_cry-_v1.7/cry.pdf.
13. Agostinelli S, Allison J, Amako K, Apostolakis J, Araujo H, Arce P, Zschiesche D. 2003 GEANT4—A simulation toolkit. *Nucl. Instrum. Methods Phys. Res. A, Accel. Spectrom. Detect. Assoc. Equip.*, **506**, 250–303. (doi:10.1016/S0168-9002(03)01368-8)